AWESW2022
21st Australasian Wind Engineering Society Workshop
2 – 3 February, 2023

# Numerical and experimental study on the pressure development in gable roof buildings having different roof pitches under perpendicular and oblique wind directions

Fengda Xing [1], Kasun Wijesooriya [2], Damith Mohotti[2*], Priyan Mendis[3]

[1]*School of Civil Engineering, Faculty of Engineering, The University of Sydney, Darlington NSW 2006, Australia.*
[2]*School of Engineering and Information Technology, The University of New South Wales, Canberra, ACT 2600, Australia.*
[3]*Department of Infrastructure Engineering, The University of Melbourne, Melbourne 3010, Australia*
**Corresponding author. E-mail: d.mohotti@unsw.edu.au.*

## ABSTRACT

Localised pressures induced by strong winds are often critical in low-rise structures such as gable roofed warehouses, especially under oblique wind directions. This study investigates the mean pressure distributions around gable roof buildings. Tests on three different roof pitches of 1:5, 2:5 and 3:5 were Investigated. Wind tunnel tests, 3D steady Reynolds-averaged Navier-Stokes (RANS) and large eddy simulation (LES) were critically compared. Under perpendicular wind attack angles, intense flow separation is observed on the roof with a lower roof pitch due to the sharp edge. Under oblique wind directions, conical vortices occur and lead to high suction areas, mainly on the long leading edge, short leading edge and roof ridge. There is a general tendency for high suctions to reduce significantly when the roof pitch becomes steeper. It is observed that when the buildings are subjected to perpendicular wind directions, simulation results from RANS show good agreement with the experimental results. However, at oblique wind attack angles, RANS simulations are incapable of reproducing vortices that occur at roof corners and long leading edges. It is noted that a scale-resolving turbulence model such as LES is required to reproduce complex flow features.

## 1. Introduction

Wind loading is one of the most critical factors in designing a low-rise building such as a gable-roofed warehouse. Many parameters, such as wind direction and building geometry, can affect the localised pressure on the building's surface. Under oblique wind attack angles, conical vortices are generated and lead to large suctions on the roof, which may cause severe damage and should be given sufficient attention during building design. Previous studies related to conical vortices on different building geometries can be found, such as a flat roof building (Tryggeson and Lyberg, 2010), curved roof building (Franchini et al., 2005), and saddle roof building (Dong and Ye, 2012). The motion of corner vortices has been proven to be closely related to the wind direction. Roof pitch is a well-known factor among the various parameters related to building geometry and has been extensively investigated over the last several decades. Hoxey et al. (1993) summarised that the pressure changes brought by building geometries were not reflected in current wind loading design codes after investigating gable roof models with roof angles of 14° and 26°. Xu and Reardon (1998) found that the 30° hip roof had the highest suction pressure at the roof corner compared to the other two hipped roof models having 15° and 20° roof angles. A more comprehensive study was later conducted by Prasad et al. (2009), who

considered gable, hipped and flat-roof buildings. They found that gable and hipped roof buildings having a critical roof angle of 45° had the least peak suction pressures on the roof compared to the other roof angles. In the above studies related to roof pitch, only perpendicular wind directions were considered, and the conical vortices resulted from oblique wind direction were not included. The influence of roof pitch on the wind flow around low-rise buildings under both perpendicular and oblique wind directions has rarely been investigated. It is necessary to conduct a more comprehensive study to identify the critical areas, especially the high suction areas of a low-rise building having different roof pitches under various wind directions, which is of great importance for building design.
The study presented in this paper concentrates on the variation of pressure distribution brought by different wind directions around three gable roof models having three roof pitches of 1:5, 2:5 and 3:5, respectively. A boundary layer wind tunnel is used in this study in conjunction with numerical simulations performed with steady Reynolds-averaged Navier-Stokes (RANS) simulation and large eddy simulation (LES).

## 2. Experimental Setup

The experiments were carried out in the Boundary Layer Wind Tunnel within the school of civil engineering at the University of Sydney. The test section of the boundary layer wind tunnel is 20 m long, 2.5 m wide, and 2 m high. The atmospheric boundary layer was created by a combination of spires and grass carpets. The building models having roof pitches of 1:5, 2:5 and 3:5 was constructed from plywood with smooth surfaces, as shown in Figure 1(a). Different wind attack angles could be achieved by rotating the turn table. The wind direction is defined as 0° when the direction is parallel to the roof ridge and 90° when the direction is perpendicular to the roof ridge, as shown in Figure 1(a). Seven directions were investigated in this study, ranging from 0° to 90° at 15° intervals. The building models were made at a scale of 1:20, and the height of the eave $H$ was kept constant for all the models. A total of 90 pressure taps were used on the external surfaces, and the pressure tap distribution is shown in Figure 1(b). The same pressure tap distributions were utilised for the other three models. The mean wind velocity and turbulence intensity of the approaching flow was measured with a hot-wire probe. Time averaging was conducted for a period of 120 s with a sampling rate of 1000 Hz. The mean wind velocity and turbulence intensity measure from experiments is used as the simulation inlet conditions of this study. The aerodynamic roughness length was estimated to be 0.0003 m (0.006 m in full-scale), corresponding to open terrain conditions according to Australian Wind Standard AS 1170.2 (Committee, 2011). The reference point was selected at the height of the building eave ($H_{ref} = H$), with the reference mean velocity $U_{ref} = 8.5\ m/s$ and a reference turbulence intensity of 19%.

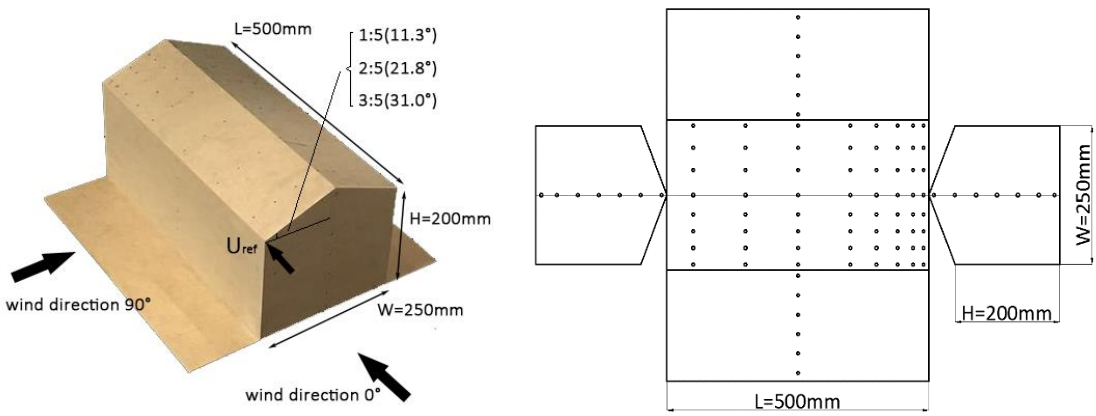


Figure 1. (a) Schematic view of the model and (b) Pressure tap distributions on the external surfaces.

## 3. Simulation Setup

ANSYS FLUENT version 18 (Fluent, 2009) was used in this study to perform the steady RANS and LES computations. The building models were created according to the sizes of the models used in the wind tunnel tests. The distances were 3H (0.825 m) from the building model to the top and the sides of the domain and 15H (4.125 m) for the downstream length, where H (0.275 m) was the height of the tallest building in this study. All the blockage ratios were below 3% for different roof pitches with this domain shape. The inlet conditions in the simulation were imposed based on wind tunnel measurements, and Symmetry boundary conditions were imposed on the sides and top of the domain. The 3D steady RANS equations are solved in combination with the $k-\omega$ shear stress transport (SST) turbulence model. The SIMPLE algorithm is used for pressure-velocity coupling. The pressure interpolation is of second order and a second-order upwind scheme discretises all the other transport equations. Convergence is obtained when the scaled residuals level off and reach a minimum of $10^{-5}$ for all dependent variables. The dynamic Smagorinsky-Lilly model is selected as the sub-grid scale model to perform LES simulation. The SIMPLE algorithm is also used for pressure-velocity coupling. The pressure interpolation is of second-order and a bounded central differencing scheme is applied to discretise the momentum equation. Bounded second-order implicit is used for transient formulation. Tetrahedral and hexahedral elements are used near and away from the building, respectively. Additionally, prism elements are imposed near solid boundaries to capture boundary layers, as shown in Figure 2. After a series of sensitivity tests, the mesh details used for RANS LES are displayed in Table 1. All the LES simulations were performed with a time step size of $6 \times 10^{-5}$ s and a sampling duration of 2 s. Due to the page limit, details about sensitivity tests are not presented in the paper and can be found in the authors' previous study (Xing et al., 2018b).

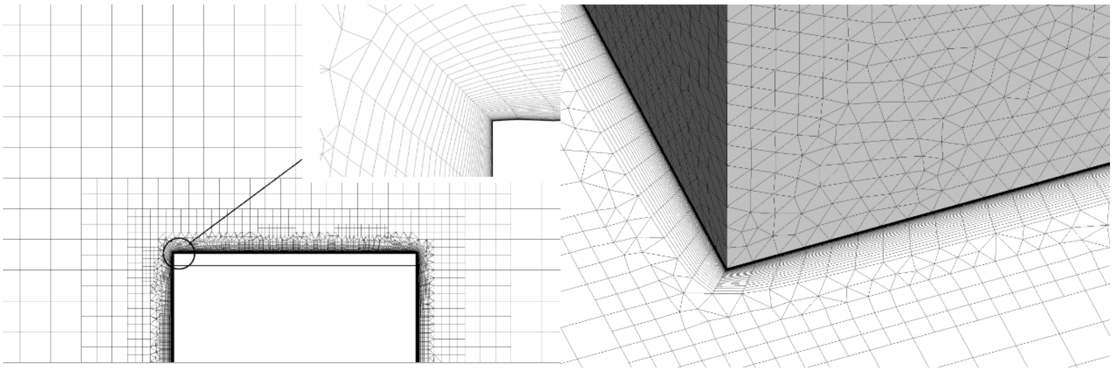

(a) (b)

Figure 2. Mesh details (a) on the longitudinal cross-plane around the building and (b) near the building corner.

Table 1. Mesh details for RANS and LES

| | Maximum mesh size (m) | Minimum mesh size (m) | First grid height of inflation layer (m) | Stretch ratio of inflation layer | Average $y^+$ around building | Total mesh number |
|---|---|---|---|---|---|---|
| RANS | 0.05 | 0.005 | 0.00002 | 1.1 | 0.2 | 703,000 |
| LES | 0.05 | 0.005 | 0.00006 | 1.2 | 0.8 | 451,000 |

## 4. Results

### *4.1 Perpendicular wind direction 90°*

In Figure 3, numerical results obtained from the $k-\omega$ SST turbulence model and the experimental results measured from the wind tunnel tests are compared on building models under a wind direction of 90°. The x-axis is the dimensionless distance along the mid-line of the building model, and the y-axis is the corresponding pressure coefficient. Generally, simulation results show good agreement with the experimental results, especially on the roof, which is a critical zone due to flow separation. Except for some underestimation of line D in the leeward part of the building with a roof pitch of 3:5, CFD has good performance in all other parts using the $k-\omega$ SST turbulence model. The positive pressure coefficient in line A of the windward wall and the absolute value of the negative pressure coefficient in line D of the leeward wall slightly increase with the roof pitch becoming steeper. However, the variations are minimal compared to the significant changes in the pressure coefficient on the roof. On the upwind roof, the absolute values of the suction pressure reduce a lot with the roof pitch gradually increasing. In addition, the pressure coefficient on the downwind roof changes into a relatively constant value of around -0.5 when the roof pitch rises from 1:5 to 2:5 and 3:5.

The different distributions of pressure coefficient in Figure 3 result from the flow separation variation intensity, which can be reflected by plotting the vorticity distribution on the mid-plane as displayed in Figure 4. Vorticity is defined as the curl of the velocity vector ($\nabla \times \vec{v}$) and is regarded as a good indicator to reflect the complexity of flow structure. It is observed in Figure 4 that the vorticity of flow separation close to the sharp edge significantly reduces with the increase of roof pitch. This indicates that a more intense flow separation can happen on the roof with a lower roof pitch due to the sharp edge. In addition, two areas with high vorticities behind the roof ridges are observed on the downwind roof in Figure 4(b, c).

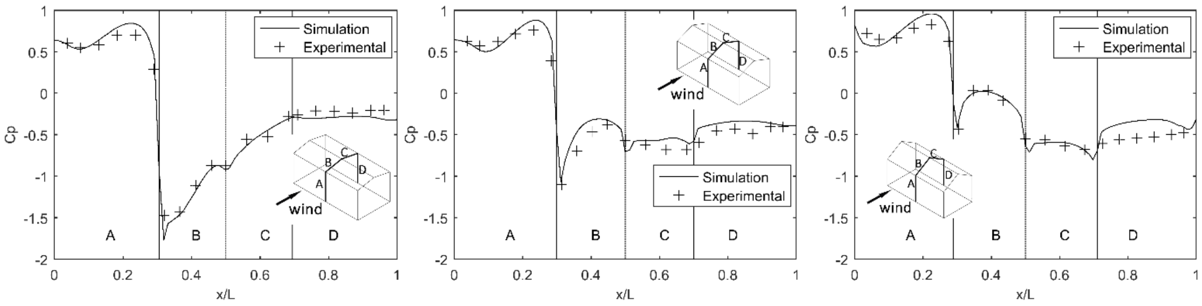

Figure 3. Pressure coefficient comparison between results from the simulation and wind tunnel test on buildings under wind direction 90° with a roof pitch of (a) 1:5, (b) 2:5, (c) 3:5.

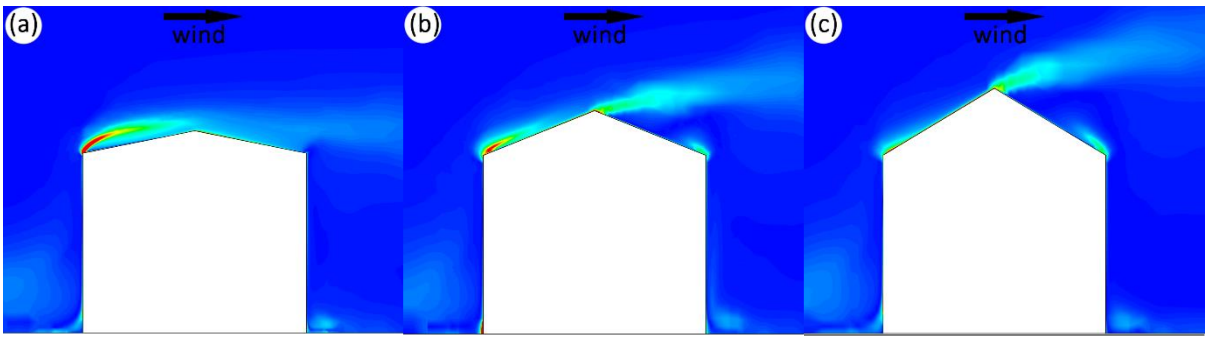

Figure 4. Vorticity distributions along the mid-planes around buildings under wind direction 90° with a roof pitch of (a) 1:5, (b) 2:5, (c) 3:5.

## *4.2 Oblique wind directions*

The pressure distribution contours on the roof with pitches of 1:5, 2:5 and 3:5 is displayed in Figure 5 under different wind directions. These contours are plotted based on the data obtained from wind tunnel tests. It is seen that the position of the high suction area changes significantly with wind direction. Generally, there is a tendency for the high suction areas on the roof to become less critical with increasing roof pitches. A critical area with an extremely low-pressure coefficient of -2 is seen on the front roof ridge with a roof pitch of 1:5 under wind direction 45°. When the roof pitch is raised to 3:5, the lowest pressure coefficient is around -1.2 under wind direction 15°, and most areas have a relatively higher-pressure coefficient of around -0.5 or greater under various wind directions. The roof pitch is proven to influence the intensity of vortices on the roof significantly. For a low roof pitch building, the contact edges between walls and roof are shaper than a higher roof pitch, which will lead to a stronger flow separation and intensify the formation of vortices on the roof (Xing et al., 2018b). Besides, the high suction areas mainly concentrate on the leading edge, short leading edge and the front part of roof ridge due to the formation of roof corner vortices.

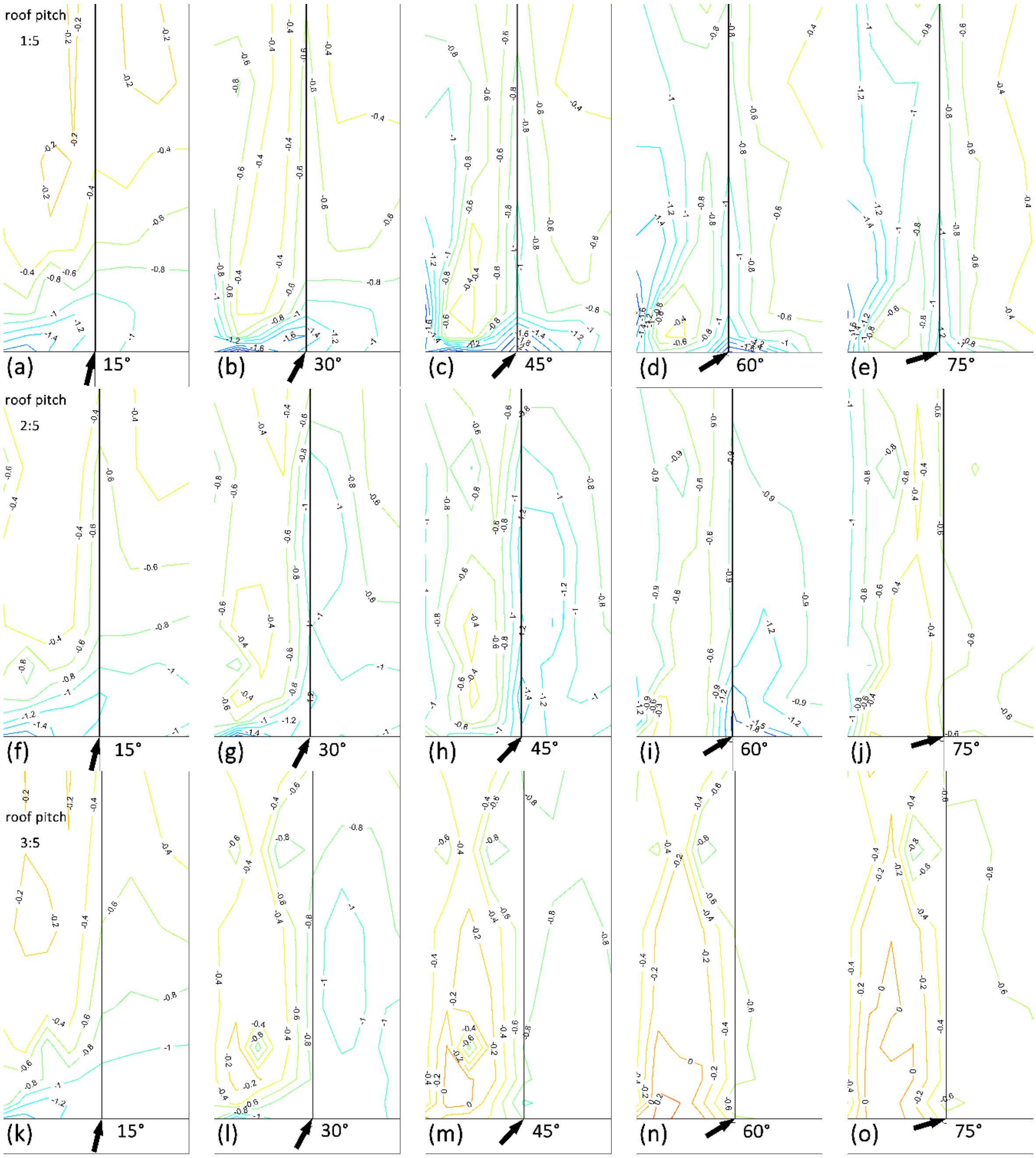


Figure 5. Pressure coefficient contours under five different wind directions for buildings with a roof pitch of (a, b, c, d, e) 1:5; (f, g, h, i, j) 2:5; (k, l, m, n, o) 3:5.

### *4.3 Comparison between RANS and LES*

The different performances between LES and RANS are evaluated by tracking the development of velocity vector in the near-building flow region around the building with a roof pitch of 1:5 under a wind direction of 60° as displayed in Figure 6. It is clearly observed in Figure 6(a) that two vortices form along the leading edge and short leading edge respectively. The vortices have certain angles with the leading edges. Besides, wind streamlines separate when flowing over the sharp edges, generating flow separation regions as observed in Figure 6(a). However, a large discrepancy can be found between LES and RANS in the generation of near-building flow regions as shown in Figure 6(b). Although RANS could create flow separations near the sharp edges, the vortex along the long leading edge is not clearly produced. The vortex size along the short leading edge is also significantly smaller compared to Figure 6(a), and the distribution tends to be parallel to the leading edge. A detailed comparison between RANS and LES results can be found in the authors' previous studies (Xing et al., 2018a, 2018b), and it is shown that LES performs better in both the generation of flow structures around buildings and the prediction of localised pressure coefficient compared to RANS.

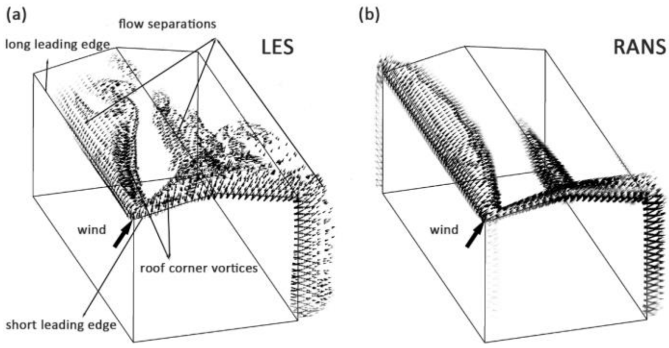


Figure 6. The developments of velocity vector on the roof generated by: (a) LES, (b) RANS.

## 4. Conclusions

This paper investigates the mean pressure distributions around gable roof buildings with three different roof pitches of 1:5, 2:5 and 3:5 by wind tunnel tests, 3D RANS and LES. Simulation results from RANS show good agreement with the experimental results when the buildings are under perpendicular directions. When the building is under oblique wind directions, high suction areas brought by conical vortices mainly concentrate on the long leading edge, short leading edge and roof ridge. There is a general tendency for high suctions to reduce significantly when the roof pitch becomes steeper. LES performs better in the simulation of roof corner vortices compared to RANS.

## References

J. T. Committee. (2011). AS/NZS 1170.2: 2011 Structural design actions-Part 2: Wind actions. *Australian/New Zealand Standard (AS/NZS): Joint Technical Committee BD-006, Australia/New Zealand*.

X. Dong, & J. Ye. (2012). The point and area-averaged wind pressure influenced by conical vortices on saddle roofs. *Journal of Wind Engineering and Industrial Aerodynamics, 101*, 67-84.

A. Fluent. (2009). 12.0 Theory Guide. *Ansys Inc, 5*.

S. Franchini, S. Pindado, J. Meseguer, & A. Sanz-Andrés. (2005). A parametric, experimental analysis of conical vortices on curved roofs of low-rise buildings. *Journal of Wind Engineering and Industrial Aerodynamics, 93*(8), 639-650.

R. Hoxey, A. Robertson, B. Basara, & B. Younis. (1993). Geometric parameters that affect wind loads on low-rise buildings: full-scale and CFD experiments. *Journal of Wind Engineering and Industrial Aerodynamics, 50*, 243-252.

D. Prasad, T. Uliate, & M. R. Ahmed. (2009). Wind loads on low-rise building models with different roof configurations. *International Journal of Fluid Mechanics Research, 36*(3).

H. Tryggeson, & M. D. Lyberg. (2010). Stationary vortices attached to flat roofs. *Journal of Wind Engineering and Industrial Aerodynamics, 98*(1), 47-54.

F. Xing, D. Mohotti, K. J. B. Chauhan, & Environment. (2018a). Experimental and numerical study on mean pressure distributions around an isolated gable roof building with and without openings. *132*, 30-44.

F. Xing, D. Mohotti, K. J. B. Chauhan, & Environment. (2018b). Study on localised wind pressure development in gable roof buildings having different roof pitches with experiments, RANS and LES simulation models. *143*, 240-257.

Y. Xu, & G. Reardon. (1998). Variations of wind pressure on hip roofs with roof pitch. *Journal of Wind Engineering and Industrial Aerodynamics, 73*(3), 267-284.